



Hot spots and hot moments of greenhouse gas emissions in agricultural peatlands

Tyler L. Anthony · Whendee L. Silver

Received: 29 May 2023 / Accepted: 20 October 2023 / Published online: 6 November 2023
© The Author(s) 2023

Abstract Drained agricultural peatlands occupy only 1% of agricultural land but are estimated to be responsible for approximately one third of global cropland greenhouse gas emissions. However, recent studies show that greenhouse gases fluxes from agricultural peatlands can vary by orders of magnitude over time. The relationship between these hot moments (individual fluxes with disproportionate impact on annual budgets) of greenhouse gas emissions and individual chamber locations (i.e. hot spots with disproportionate observations of hot moments) is poorly understood, but may help elucidate patterns and drivers of high greenhouse gas emissions from agricultural peatland soils. We used continuous chamber-based flux measurements across three land uses (corn, alfalfa, and pasture) to quantify the spatiotemporal patterns of soil greenhouse gas emissions from temperate agricultural peatlands in the Sacramento-San Joaquin Delta of California. We found that the location of hot spots of emissions varied over time

and were not consistent across annual timescales. Hot moments of nitrous oxide (N₂O) and carbon dioxide (CO₂) fluxes were more evenly distributed across space than methane (CH₄). In the corn system, hot moments of CH₄ flux were often isolated to a single location but locations were not consistent across years. Spatiotemporal variability in soil moisture, soil oxygen, and temperature helped explain patterns in N₂O fluxes in the annual corn agroecosystem but were less informative for perennial alfalfa N₂O fluxes or CH₄ fluxes across ecosystems, potentially due to insufficient spatiotemporal resolution of the associated drivers. Overall, our results do not support the concept of persistent hot spots of soil CO₂, CH₄, and N₂O emissions in these drained agricultural peatlands. Hot moments of high flux events generally varied in space and time and thus required high sample densities. Our results highlight the importance of constraining hot moments and their controls to better quantify ecosystem greenhouse gas budgets.

Responsible Editor :Klaus Butterbach-Bahl

Supplementary Information The online version contains supplementary material available at <https://doi.org/10.1007/s10533-023-01095-y>.

T. L. Anthony (✉) · W. L. Silver
Department of Environmental Science, Policy
and Management, University of California Berkeley, 130
Mulford Hall, Berkeley, CA 94720, USA
e-mail: t.anthony@berkeley.edu

Keywords Hot spots · Hot moments · Agricultural peatlands · Peatlands · Greenhouse gas fluxes · Nitrous oxide · Methane · Carbon dioxide · Soil fluxes

Introduction

Drained agricultural peatlands are characterized by some of the highest greenhouse gas emissions from

terrestrial ecosystems due to soils that are often rich in organic carbon (C) and nitrogen (N) content (Leifeld and Menichetti 2018; Hemes et al. 2019; Anthony and Silver 2020; Anthony et al. 2023). The oxidation of soil organic C to carbon dioxide (CO₂) during drainage drives the majority of the global warming potential (GWP) from agricultural peatland soils (Freeman et al. 2022). However, nitrous oxide (N₂O) and methane (CH₄) can represent up to 35% of CO₂-equivalent (CO₂e) agricultural peatland emissions (Anthony and Silver 2021). Combined agricultural peatland CO₂, N₂O and CH₄ emissions are estimated to contribute to 32% of global cropland emissions while accounting for only 3% of global land area and providing only 1% of crop kilocalories worldwide (Carlson et al. 2017; Freeman et al. 2022).

Soil N₂O and CH₄ emissions are often characterized by hot moments, where the majority of annual emissions occur on a timescale of days to weeks (Molodovskaya et al. 2012; Savage et al. 2014; Krichels and Yang 2019; Anthony and Silver 2021; Anthony et al. 2023). Hot moments of N₂O and CH₄ high emission events are often poorly constrained, but can be triggered by weather events (rainfall, freeze/thaw) or management induced changes (fertilization, irrigation, flooding, drainage) to the soil environment (Conrad 1989; McNicol and Silver 2014; Wagner-Riddle et al. 2017; Krichels et al. 2019a). The drivers of spatial variability in N₂O and CH₄ fluxes are even less well understood. Low lying areas, legacies of prior land use, and areas of particularly high resource availability may be important locations for high emission potential, termed hot spots, on the landscape. There are several ways in which hot spots of high fluxes may manifest in agricultural ecosystems (*sensu* McClain et al. 2003, Wagner-Riddle et al. 2020). Hot spots could be characterized by consistently high greenhouse gas emissions from a single locale or set of locales such as a drainage ditch or furrow which have near constant low or dynamic redox and high substrate availability. Alternatively, locations with periodic high flux events (*i.e.*, hot moments) may be limited to a single or few locations relative to a larger ecosystem matrix, thus linking hot spots with hot moments. Locations with a higher probability for hot moments of high flux may be characterized by microtopography (*e.g.*, low lying areas), properties of vegetation (*e.g.*, high litterfall inputs), or land use legacies (*e.g.*, N fixing crops) (Krichels and Yang 2019;

Hall et al. 2023). Finally, hot spots could occur inconsistently as locales with a higher proportion of hot moments than the surrounding matrix for a defined period (month, season, year) that vary over space and time. This final category of greenhouse gas emission hot spot would be particularly difficult to characterize but could be linked to dynamic soil heterogeneity (Totsche et al. 2010), land management activities such as tillage, planting, or fertilizer application that may reduce spatial variability in soil conditions (Adewale et al. 2016), or result from random, or chaotic processes associated with ecosystem complexity (Baveye et al. 2018; Sokol et al. 2022).

The datasets needed to constrain hot spots and hot moments of ecosystem processes are inherently large and complex. Denitrification and methanogenesis are often regulated by non-linear and interactive effects which are difficult to model using traditional approaches. Machine learning models can help capture trends and identify important drivers and predictors of ecosystem processes; relationships are determined from available data, allowing for unbiased projections while providing insights into functional relationships (Saha et al. 2021). Machine learning models can also be used to make projections at larger spatial and temporal scales (Alber et al. 2019). Supervised machine learning models, such as random forest modelling, utilize an algorithm for classification and regression based on the principle of recursive partitioning (Breiman 2001), and independent of the assumption of functional relationships between the response and predictor variables (Saha et al. 2021).

An important limitation of machine learning models is that they require large, high-quality training datasets to appropriately train the model without using a significant proportion of the observed data (Qiu et al. 2016). Accuracy likely improves with increased spatial and temporal data inputs and is therefore inherently limited by the scope of a training dataset. This makes it difficult to predict the occurrence and magnitude of hot spots and hot moments without adequate representation of large flux events within training datasets. Unexplained variability in previously developed models is likely a function of consistently underfitting hot moments or under sampling key driving variables (soil O₂, moisture, and temperature) across space or time. Continuous long-term (multi-month or year) measurements of N₂O and CH₄ fluxes and their drivers

across scales are rare, limiting our ability to scale hot spots and hot moments across time and space.

Continuous automated measurements can improve the temporal resolution of greenhouse gas emissions data (Holst et al. 2008; Barton et al. 2015). However, these approaches are still typically limited to 6–12 sampling locations and study duration is often less than one full year. Similar challenges exist for the determination of controlling variables occurring within soil environments (spatial scales from aggregate to pedon and temporal scales from seconds to days). Patterns in substrate availability, gas diffusivity, and microbial activity throughout a soil profile are likely to be important drivers of observed spatiotemporal variability in agricultural peatland greenhouse gas emissions. Soil moisture content, redox conditions, and C and nutrient availability often vary with depth in soils, leading to differential patterns in C and N cycling (Jobbagy and Jackson 2000; Krichels et al. 2019b; Thorup-Kristensen et al. 2020). Incorporating physical and biogeochemical conditions both vertically and horizontally in soils can significantly improve predictions of greenhouse gas fluxes (Potter 1997; Chatskikh et al. 2005; Xing et al. 2011; Feng et al. 2021). Thus, challenges persist for the prediction of greenhouse gas emissions at an ecosystem scale and corresponding calibration data is likely to be critical to better predict spatiotemporal variability.

In agricultural peatlands, soil nitrate (NO_3^-) availability, water filled pore space (WFPS), and its effects on O_2 availability can be significant drivers of hot moment N_2O flux events (Pärn et al. 2018; Anthony and Silver 2021; Anthony et al. 2023). Soil NO_3^- can accumulate under oxic, well-drained soil conditions via N mineralization and nitrification following fertilization or crop harvest (Kirk et al. 2015; Anthony and Silver 2021) and may be supplemented by Fe-coupled anaerobic ammonium oxidation in Fe- and C-rich peatlands soils (Martikainen et al. 1993; Golovchenko et al. 2007; Yang et al. 2012; Yang and Liptzin 2015). Due to a relatively unlimited organic C and N supply (in comparison to most other soils), many temperate agricultural peatland soils experience high rates of N mineralization and nitrification (Danevčič et al. 2010; Jerman et al. 2017; Oktarita et al. 2017) suggesting a sustained and active N cycling microbial community that likely facilitates the production and emission of N_2O .

Net CH_4 fluxes from agricultural peatlands are assumed to be minimal under drained conditions (Maljanen et al. 2010; Günther et al. 2019) as this is thought to favor aerobic respiration pathways that out-compete methanogens for available substrate and/or stimulate methanotrophic activity (Conrad 2007). But irrigation or intense rainfall events can create periods of anaerobic conditions ideal for CH_4 production (Hemes et al. 2019; Anthony and Silver 2021). At the ecosystem scale, the influence of soil temperature, water table fluctuations, and plant activity drive CH_4 fluxes in both drained and restored wetlands, often as scale emergent controls that can only be determined with high density eddy covariance measurements (Sturtevant et al. 2016; Oikawa et al. 2017; Chamberlain et al. 2018). However, spatial prediction of CH_4 fluxes often suffers from the same pitfalls as N_2O flux predictions, with methods lacking agreement between observed and predicted fluxes and poor performance when extrapolated to other locations (Ehrhardt et al. 2018; Gaillard et al. 2018).

Cover type and management are likely to be important determinants of the patterns and magnitude of greenhouse gas emissions from drained agricultural peatlands. Agriculture practices in drained peatlands are generally determined by soil organic matter content and nutrient availability, and can range from grazed pastures to annual or perennial agricultural systems (Hatala et al. 2012; Knox et al. 2015), all of which may vary in rates and pathways of greenhouse gas fluxes. In some drained temperate peatlands including California's Sacramento-San Joaquin Delta, soils with elevated organic matter content, and thus high rates of organic matter mineralization, are frequently chosen for corn (*Zea mays*) agriculture given their inherent productivity. As annual cropping systems, these ecosystems are often prioritized for winter flooding of fallow fields for weed management and migrating waterfowl habitat that also coincide with hot moments of CH_4 and N_2O flux (Pellerin et al. 2014; Anthony and Silver 2021). In contrast, more degraded peat soils with higher mineral content are often prioritized for alfalfa (*Medicago sativa*) agriculture as this perennial is an N-fixing crop and can be productive over many years with a single planting and only periodic summer irrigation (Anthony et al. 2023). The most degraded soils are often managed as ditch-irrigated grazed pasture as they are not economically suitable for crop agriculture (Teh et al.

2011; Knox et al. 2015). Drained and irrigated peatlands generally experience predictable periods of inundation followed by well-aerated conditions; this combination fosters the biogeochemical environment needed to drive high greenhouse gas fluxes (Hemes et al. 2019; Anthony and Silver 2021; Anthony et al. 2023). Dynamic redox conditions over time can support high substrate availability for both denitrifiers (e.g., higher redox) and methanogens (e.g., lower redox) (Conrad 1989). Methane and N₂O fluxes can also be supported by microtopographic variability that leads to temporary ponding in low-lying regions with gradients of reducing conditions and well-aerated environments.

To better constrain greenhouse gas budgets and their drivers from agricultural peatlands, we conducted continuous *in-situ* soil greenhouse gas flux measurements from three different agricultural peatland land uses in a small geographical area (~60 km²): an annual corn cropping system, a perennial alfalfa cropping system, and a grazed irrigated pasture. These systems provided a unique template to explore the variability in greenhouse gas fluxes across land uses while controlling for climate and general soil conditions (e.g., drained peatland). We tested the hypothesis that drained peatland agricultural creates persistent hot spots of CH₄ and N₂O emissions due to low or fluctuating redox conditions, respectively, and that the majority of hot moments would be limited to a relatively few hot spot chambers. We also hypothesized that this method of quantifying hot spots and hot moments would identify relatively less CO₂ hot spots and hot moments as soil respiration would be more uniformly distributed across these agricultural peatland ecosystems with variability driven by seasonality in temperature and precipitation. We predicted that the annual corn system would have fewer emission hot spots due more uniformity in inputs and surface soil disturbance from intensive management, while the perennial alfalfa system and pasture would have relatively greater hot spot variability due to the development of greater heterogeneity over time in the absence of intensive management. We used continuous cavity ringdown spectroscopy and automated chambers to measure CO₂, CH₄, and N₂O fluxes. Soil sensing data of O₂, moisture, and temperature across three soil depths (10, 30, and 50 cm) from the corn and alfalfa sites allowed us to explore potential drivers. Our goal was to quantify the spatiotemporal

distribution of chamber-scale hot spots and hot moments in agricultural peatlands, the relationships between hot spots and hot moments of greenhouse gas flux, and explore machine learning methods to predict these hot spots and hot moments across different agricultural peatland land uses.

Methods

Site description

We used data from three agricultural peatland sites in the Sacramento-San Joaquin Delta region of California. The sites experienced a similar climate over a relatively small regional scale (~60 km²) but had contrasting land uses and soil conditions (Table 1). The datasets included over 98,000 chamber flux measurements from an organic-rich annual maize agroecosystem (38.1091° N, 121.5351° W; hereafter referred to as corn). Preliminary data on temporal flux patterns from years 1 to 3 were reported in Anthony and Silver (2021); here we added an additional year of observations and explored spatial dynamics not previously considered. We also included data from a continuous perennial alfalfa agroecosystem (chambers: 38.1076° N, 121.5021° W, tower: 38.0992° N, 121.4993° W; hereafter referred to as alfalfa) with 103,000 flux measurements; as with the corn site previous work explored the temporal dynamics of greenhouse gas emissions from this site, but did not report spatial patterning (Anthony et al. 2023). Finally, we included data from a continuously grazed irrigated pasture 38.0402° N, – 121.7272° W; hereafter referred to as pasture) with 33,000 flux measurements. These are the three dominant land uses for drained agricultural peatlands in the region, accounting for 53% of crop acreage (The Delta Protection Commission 2020). Importantly, grazed pastures often occur on degraded peatland soils where other agricultural activity is less likely to be profitable (Hatala et al. 2012; Buschmann et al. 2020). Corn was the only system to receive N fertilizer inputs, which were applied at a rate of 118 kg N ha⁻¹ year⁻¹ (Anthony and Silver 2021). Here we used the three datasets, where we include both fluxes to the atmosphere from soil and fluxes from the atmosphere to the soil, to explore spatial dynamics both within and

Table 1 Descriptions of soil C (% ± SE), soil N (% ± SE), and soil pH (± SE) in the top 0–15 cm and relevant management information

Land use	Soil C (%)	Soil N (%)	Soil pH	Flux measurement periods	Soil sensor measurement periods	Management information
Corn: Annual maize cropping system	15.2 ± 0.4%	1.0 ± 0.02%	5.89 ± 0.05	June 2017–June 2021	October 2018–June 2021	Flooded in winter (approximately November–March) for migrating waterfowl habitat
Alfalfa: Perennial alfalfa cropping system	5.3 ± 0.02%	0.38 ± 0.01%	4.93 ± 0.04	January 2017–January 2021	October 2018–January 2021	Flood irrigated approximately once a month during from May–September
Pasture: Irrigated, grazed pasture	9.0 ± 0.1%	0.63 ± 0.01%	5.13 ± 0.07	April 2019–July 2020	April 2019–July 2020	Ditch subsurface irrigation to maintain productivity (May–September), grazed by cattle year-round

across agricultural peatland ecosystems and relationships to temporal patterns which previous studies did not address.

Greenhouse gas flux measurements

All datasets collected soil fluxes of CO₂, CH₄, and N₂O continuously using an automated chamber system for 1 to 4 years. Each system consisted of nine opaque, automated gas flux chambers (eosAC, Eosense, Nova Scotia, Canada) connected to a multiplexer (eosMX, Eosense, Nova Scotia, Canada). The multiplexer allowed for dynamically signaled chamber deployment and routed gases to a cavity ring-down spectrometer (Picarro G2508, Santa Clara, CA, USA). Chambers were measured sequentially over a 10-min sampling period with a 1.5-min flushing period before and after each measurement. Chambers were deployed in a 10 × 10 m grid design, with each chamber approximately 5 m from other chambers. Vegetation was included in all pasture chambers and randomly assigned to bare soil (n = 4) or plants (n = 5) in alfalfa. In corn, chambers were randomly assigned to beds (n = 3) or furrows (n = 6) without vegetation included due to the height of the stalks. Data filtering and detection limits are described in detail in Anthony & Silver (2021) and Anthony et al. (2023).

Site-level net ecosystem CO₂ exchange (NEE) and calculated site-level global warming potential (GWP) utilizing annual flux measurements from

paired Ameriflux towers in corn (US-Bi2) and pasture (US-Snf) sites (Kasak et al. 2020; Rey-Sanchez et al. 2021) was employed to contextualize the importance of hot moments on net ecosystem CO₂e budgets. For the alfalfa site, we utilized annual net ecosystem exchange (NEE) estimates from a nearby (< 1 km) Ameriflux tower (US-Bi1) in an alfalfa agroecosystem with identical management practices and soil type (Anthony and Silver 2020; Rey-Sanchez et al. 2022b). The eddy covariance technique captures continuous, long-term exchange of CO₂, CH₄, water, and energy fluxes between the landscape and the atmosphere, along with measurements of environmental drivers (Eichelmann et al. 2018). Fluxes were measured at a frequency of 20 Hz using open-path infrared gas analyzers (LI-7500 for CO₂, LI-7700 for CH₄, LiCOR Inc., Lincoln, NE, USA). Sonic anemometers measured sonic temperature and three-dimensional wind speed at 20 Hz (WindMaster Pro 1590, Gill Instruments Ltd, Lymington, Hampshire, England). To convert N₂O and CH₄ flux measurements to CO₂e, we used the IPCC AR5 100-year GWP values of 28 CO₂e for CH₄ and 298 CO₂e for N₂O (Myhre et al. 2013).

Environmental sensors

In both the corn and alfalfa systems, two sets of soil sensors per site were installed at depths of 10 cm, 30 cm, and 50 cm and included O₂ and soil

temperature sensors (SO-110, Apogee Instruments, Logan, UT) and moisture sensors (CS616, Campbell Scientific, Logan, UT) connected to a datalogger (CR1000, Campbell Scientific, Logan, UT) from September 2018–February 2021 in alfalfa and October 2018–July 2021 in corn. Sensors were installed as close to corresponding chamber grid locations as possible while minimizing soil disturbance and limiting interference with agricultural activities. Except for periodic agricultural events, sensors remained installed throughout the year. Data filtering and data gaps are described in detail in Anthony & Silver (2021) and Anthony et al. (2023).

Statistical analyses and machine learning

Following data filtering, annual fluxes and the quantity and magnitude of hot moments and hot spots were determined. Annual fluxes were determined by taking the mean annual flux of each chamber as well as the mean annual flux for each field location. We defined hot moments as flux measurements with values greater than four standard deviations from the mean (Anthony and Silver 2021; Anthony et al. 2023), as statistically 99.9% of the population should fall within four standard deviations of the mean given a normally-distributed dataset. All individual flux datasets (CO_2 , CH_4 , and N_2O) from each field site were approximately log-normally distributed. Calculating standard deviations on non-Gaussian datasets generally overestimates the true standard deviation (Carter 2013), but is still appropriate in describing the spread of the variable of interest. Therefore, quantifying hot moments in this manner is generally conservative, as using an inflated standard deviation quantifies individual flux observations that are significantly outside the range of expected observations. Determining the variation across datasets can provide a metric to compare how moments vary across fluxes (CO_2 , CH_4 , and N_2O) and across ecosystem. We defined a hot spot as any individual chamber with greater than 11% of hot moment observations within an annual flux dataset. This metric was chosen because if hot moments were evenly distributed across chambers, each chamber would represent 11% of hot moment observations. Therefore, any hot spot chamber with greater than 11% of hot moment observations would thus disproportionately contribute to the total ecosystem flux. Spatiotemporal differences in hot spots were

tested with two-way analysis of variance (ANOVA) of annual mean greenhouse across chambers and site-years for each location.

The greenhouse gas flux and soil sensor datasets (corn and alfalfa only) were collected with sufficient spatiotemporal frequency to utilize machine learning approaches to determine drivers of N_2O and CH_4 fluxes. We used a random forest machine learning model (Hamrani et al. 2020; Saha et al. 2021) for both datasets separately to determine if increased sampling density can predict N_2O and CH_4 fluxes. Input variables included individual observations of N_2O and CH_4 fluxes and volumetric water content (VWC), O_2 , and temperature across a soil profile (10, 30, and 50 cm) as predictor variables. As sensors were not deployed with each individual chamber, some spatial resolution could not be accounted for with sensor observations. The relative importance of each input variable in the machine learning models were determined by utilizing a node impurity measure, which is related to the corresponding response variance in the variable of interest (Segal and Xiao 2011).

Results

Spatiotemporal patterns in emissions across ecosystems

The three land uses differed in patterns of greenhouse gas emissions and net ecosystem exchange (Table 2). The alfalfa and pasture were net CO_2e sinks over the study periods. The corn had mean annual emissions of $46.7 \pm 0.8 \text{ Mg CO}_2\text{e ha}^{-1} \text{ year}^{-1}$ with CO_2 accounting for 58.0% of this, followed by 34.9% as N_2O and 7.1% as CH_4 . Together, the average annual GWP of N_2O plus CH_4 was $19.6 \pm 0.8 \text{ Mg CO}_2\text{e ha}^{-1} \text{ year}^{-1}$ (Table 2). The alfalfa site was on average a net CO_2e sink of $-23.3 \pm 0.5 \text{ Mg CO}_2\text{e ha}^{-1} \text{ year}^{-1}$. Soil N_2O emissions decreased the net CO_2e sink by 8.0% and the average GWP of N_2O plus CH_4 was $1.84 \pm 0.01 \text{ Mg CO}_2\text{e ha}^{-1} \text{ year}^{-1}$. The pasture site had the lowest annual fluxes with $-9.66 \pm 0.11 \text{ Mg CO}_2\text{e ha}^{-1} \text{ year}^{-1}$, with N_2O decreasing the net CO_2e sink by 12.8% and an average GWP of N_2O plus CH_4 of $1.54 \pm 0.11 \text{ Mg CO}_2\text{e ha}^{-1} \text{ year}^{-1}$.

The frequency of hot moments varied by site. In the corn, hot moments of N_2O and CH_4 emissions represented 1.1 ± 0.2 and $1.3 \pm 0.2\%$ of

Table 2 Annual mean [ecosystem respiration (R_{eco})] ecosystem exchange (NEE) and GWP from N_2O , CH_4 , and total net ecosystem carbon dioxide equivalent (CO_2e) budgets by site

Site	R_{eco} ($\text{Mg CO}_2 \text{ ha}^{-1} \text{ year}^{-1}$)	NEE CO_2 ($\text{Mg CO}_2 \text{ ha}^{-1} \text{ year}^{-1}$)	N_2O ($\text{Mg CO}_2\text{e ha}^{-1} \text{ year}^{-1}$)	CH_4 ($\text{kg CO}_2\text{e ha}^{-1} \text{ year}^{-1}$)	Total ($\text{Mg CO}_2\text{e ha}^{-1} \text{ year}^{-1}$)
Corn	66.1 ± 0.04	27.1 ± 0.02	16.3 ± 0.4	$3,300 \pm 700$	46.7 ± 0.1
Alfalfa	64.5 ± 0.1	-23.3 ± 0.5	1.86 ± 0.01	-15 ± 1	-21.2 ± 0.5
Pasture	70.2 ± 0.3	-11.10 ± 0.01	1.55 ± 0.03	-0.11 ± 0.11	-9.66 ± 0.01

Note that this analysis does not account for removed biomass from harvest or grazing

measurements, respectively, but contributed to $45 \pm 1\%$ of annual N_2O fluxes and to $140 \pm 9\%$ of annual CH_4 fluxes. In the alfalfa system hot moments of N_2O emissions were only $0.1 \pm 0.05\%$ of annual measurements but were $31.6 \pm 0.2\%$ of the annual flux (Anthony et al. 2023). The alfalfa ecosystem did not experience significant changes in annual CH_4 budgets from either hot spots or hot moments and overall was a small net CH_4 sink (Fig. 4, middle). In the grazed pasture, hot moments of N_2O flux accounted for 22% of total N_2O emissions but were again less than 1% of measurements. Hot moments of CH_4 flux were only 0.3% of fluxes but decreased the net CH_4 sink by 53% (from -24.1 to $-11.3 \text{ g m}^{-2} \text{ year}^{-1}$). Hot moments of CO_2 emissions consistently contributed less to overall fluxes than hot moments of N_2O or CH_4 . Hot moments of CO_2 emissions were of the greatest importance to the total ecosystem GWP flux in the pasture ecosystem relative to the corn or alfalfa. In the pasture only 1.0% of CO_2 flux measurements

represented 5.4% of net CO_2 emissions (Figure S6, top). In the corn system, CO_2 hot moments were only 0.4% of observations but represented 4.3% of net CO_2 emissions (Figure S4, top). Hot moments of CO_2 fluxes were the lowest percent of total emissions in the alfalfa system, with hot moments representing 0.5% of measurements but 2% of net CO_2 emissions (Figure S5, top).

Hot spots of greenhouse gas emissions across ecosystems

We used the individual chamber measurements to explore the spatial and temporal distribution of hot spots of greenhouse gas emissions across time. Across all three field sites, no individual chamber was consistently a hot spot of CO_2 , CH_4 , or N_2O emissions on annual timescales (Figs. 1, 2, 3). We found significant temporal variability in the magnitude of greenhouse gas fluxes both within and cross chamber locations

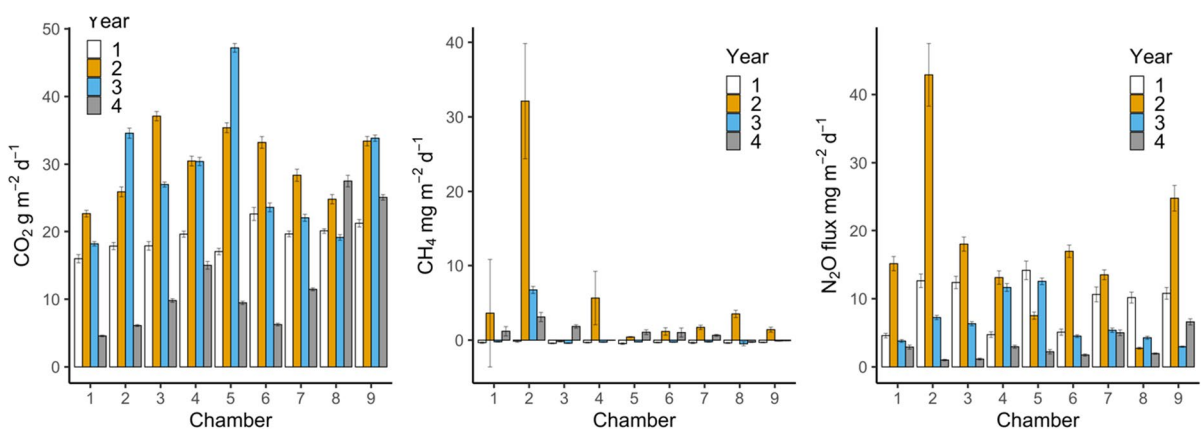


Fig. 1 Annual mean (\pm standard error) (left) CO_2 ($\text{g CO}_2 \text{ m}^{-2} \text{ day}^{-1}$), (middle) CH_4 ($\text{mg CH}_4 \text{ m}^{-2} \text{ day}^{-1}$), and (right) N_2O ($\text{mg N}_2\text{O m}^{-2} \text{ day}^{-1}$) fluxes by chamber from an annual corn agricultural peatland from June 2017 through June 2021.

White, orange, blue, and gray bars are annual mean flux measurements with black error bars representing annual standard error

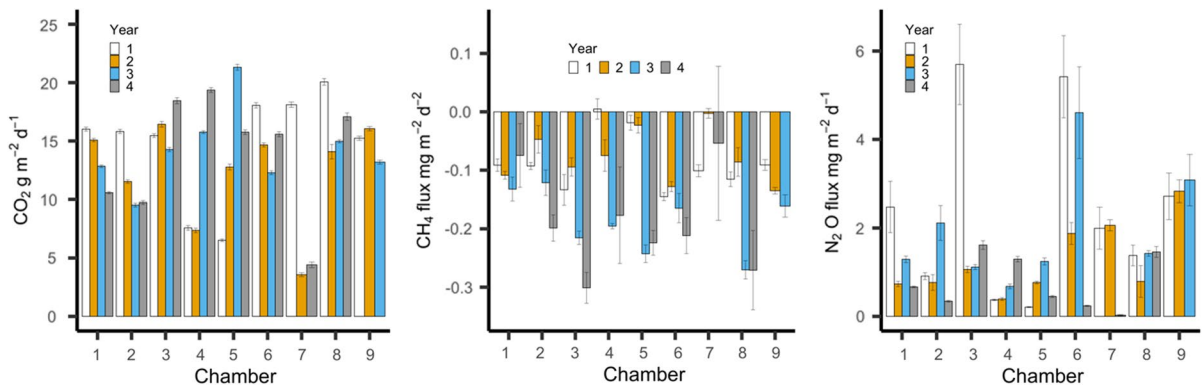


Fig. 2 Annual mean (\pm standard error) (left) CO_2 ($\text{g CO}_2 \text{ m}^{-2} \text{ day}^{-1}$), (middle) CH_4 ($\text{mg CH}_4 \text{ m}^{-2} \text{ day}^{-1}$), and (right) N_2O ($\text{mg N}_2\text{O m}^{-2} \text{ day}^{-1}$) fluxes by chamber from a perennial alfalfa agricultural peatland January 2017 through January

2021. White, orange, blue, and gray bars are annual mean flux measurements with black error bars representing annual standard error

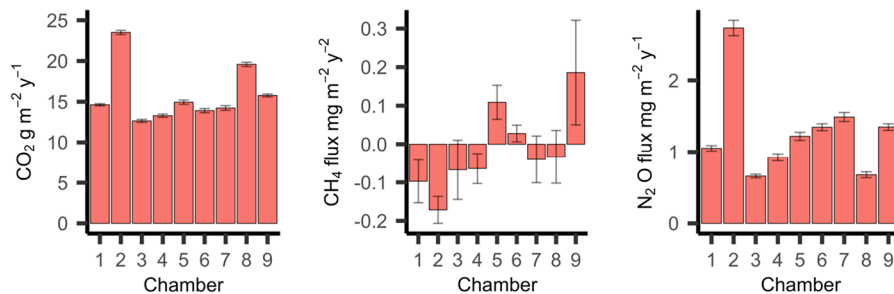


Fig. 3 Annual mean (\pm standard error) (left) CO_2 ($\text{g CO}_2 \text{ m}^{-2} \text{ day}^{-1}$), (middle) CH_4 ($\text{mg CH}_4 \text{ m}^{-2} \text{ day}^{-1}$), and (right) N_2O ($\text{mg N}_2\text{O m}^{-2} \text{ day}^{-1}$) fluxes by chamber from a grazed

pasture agricultural peatland April 2019 through April 2020. Red bars are annual mean flux measurements with black error bars representing annual standard error

($p < 0.001$, Figs. 1, 2, 3). For CO_2 , the corn site had four chambers with over 11% of hot moments, with the highest at 19.8% followed by 19.1%, 16.9%, and 14.3%. On an annual basis, the location of hot spot chambers varied across years. There were also four chambers were over 11% of the CO_2 flux in alfalfa, with one hot spot representing 27.5% of all hot moment observations, followed by 21.1%, 16.4%, and 12.6% in the other chambers; hot spot chambers also varied over time on an annual time scale. The pasture site only had two chambers over 11% of the CO_2 flux, with one chamber representing 65.6% of all hot moments, followed by 11.4% of observations in the other chamber. Importantly, all chambers exhibited individual hot moments of CO_2 flux in both the corn and alfalfa site, while two of the nine chambers in the pasture site had no hot moments observations.

However, hot moments of CO_2 flux were not significant proportions of total CO_2 soil flux budgets, representing a maximum of only 4% of annual soil CO_2 fluxes.

The relative contribution of hot spots to N_2O hot moment fluxes was similar to the distribution for CO_2 hot spots in all three sites, with the largest individual hot moment observations for both CO_2 and N_2O observed in the same chambers. Hot moments of N_2O emissions were relatively common, with the majority of chambers exhibiting hot moments of N_2O fluxes in all three agroecosystems (Fig. 5). There were individual locations with higher annual N_2O fluxes than all other chambers, but hot moments of N_2O flux were observed across multiple chamber locations (Fig. 1, 2, 3). In the corn site the highest contribution was 19.1% of N_2O hot moments from one chamber, followed

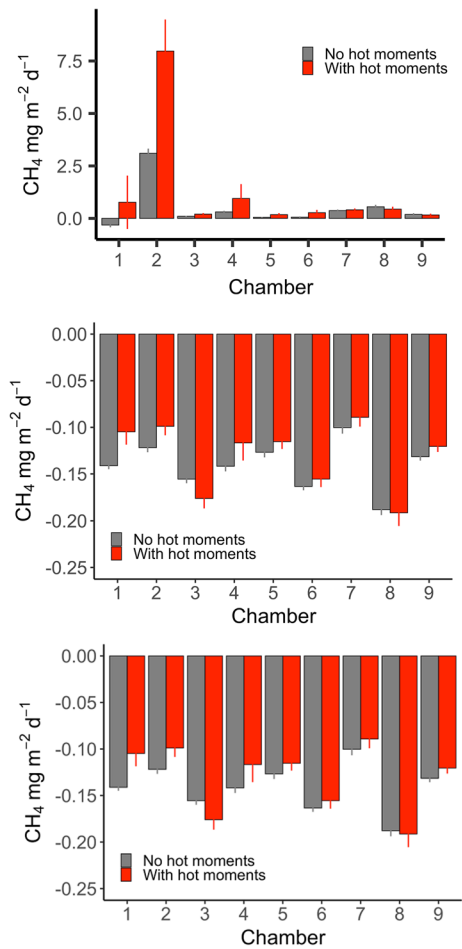


Fig. 4 Annual mean (\pm standard error) CH₄ (mg CH₄ m⁻² day⁻¹) fluxes with and without hot moments by chamber from an (top) annual corn agricultural peatland from June 2017 through June 2021, (middle) a perennial alfalfa agricultural peatland from January 2017 through February 2021, and (bottom) a grazed pasture agricultural peatland from April 2019 through June 2020

by 16.6%, 14.0%, 12.9%, and 11.6% from four other chambers with over 11% of the hot moments. There were only three chambers with greater than 11% of N₂O hot moment observations in the alfalfa site, with a single hot spot representing 32.8% of observations (followed by 22.9% and 16.4%, respectively). At the pasture site, a single hot spot represented 68.5% of N₂O hot moments from one chamber that was also the largest contribution to CO₂ hot spots.

Most CH₄ hot moments were generally focused in one location. In the corn site, 57.3% of all CH₄ hot moment fluxes occurred in only one chamber, with all

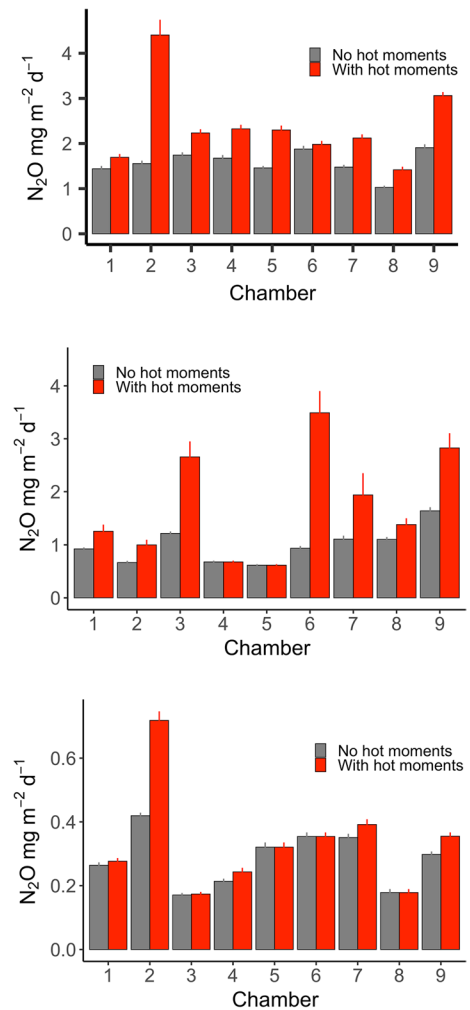


Fig. 5 Annual mean (\pm standard error) N₂O (mg N₂O m⁻² day⁻¹) fluxes with and without hot moments by chamber from an (top) annual corn agricultural peatland from June 2017 through June 2021, (middle) a perennial alfalfa agricultural peatland from January 2017 through February 2021, and (bottom) a grazed pasture agricultural peatland from April 2019 through June 2020

other chambers accounted for less than 11% of total hot moment observations. Alfalfa and pasture sites had similar distributions of CH₄ hot spots. In alfalfa, 33.3% of hot moments were observed from one chamber, followed by 15.3% and 13.6% in two other chambers while in the pasture site 24% of hot moments from one chamber with only two other chambers over 11% of observations, at 21.3% and 16%, respectively. In the corn site hot moments of CH₄ flux were predominantly driven by fluxes from a single location

that contributed disproportionately to a net ecosystem CH_4 flux (i.e. a hot spot, Fig. 4). In contrast, in the perennial alfalfa and grazed pasture systems, CH_4 hot spots only had a small impact on the net CH_4 sink (Fig. 4).

Machine learning predictions of nitrous oxide and methane fluxes

A machine learning model using the corn flux and sensor dataset was able to account for 81% of the variance observed in N_2O fluxes with soil VWC, O_2 , and temperature sensor data across depths (10, 30, and 50 cm) (Fig. 6). Node impurity measurements suggested both VWC and temperature across depths had the highest relative importance in determining N_2O fluxes. With the alfalfa agroecosystem dataset, a machine learning model was only able to account for 16% of the variance observed in N_2O fluxes (Fig. 6) and soil O_2 , VWC, and temperature all had similar

values of relative importance. Both the alfalfa and corn machine learning models systematically underfit the largest N_2O fluxes (Fig. 6). For CH_4 fluxes, machine learning performed significantly worse. The models were only able to account for 24% of the variance in the annual corn cropping system and 6% of the variance in the perennial alfalfa cropping system (Fig. 7).

Discussion

The relationship between hot spots and hot moments of emissions

Hot spots of greenhouse gas emissions can be characterized in several ways: as sites with consistently high emissions, sites with a higher proportion of hot moments than the surrounding matrix, or locations with high emissions for a defined period (month,

Fig. 6 Comparison of observed N_2O fluxes ($\text{nmol m}^{-2} \text{s}^{-1}$) to machine learning predicted N_2O fluxes ($\text{nmol m}^{-2} \text{s}^{-1}$) from agricultural peatland corn (a) and (b) alfalfa agroecosystems. Predictor variables were identical for each ecosystem (10, 30, and 50 cm depths with oxygen, moisture, and temperature sensors)

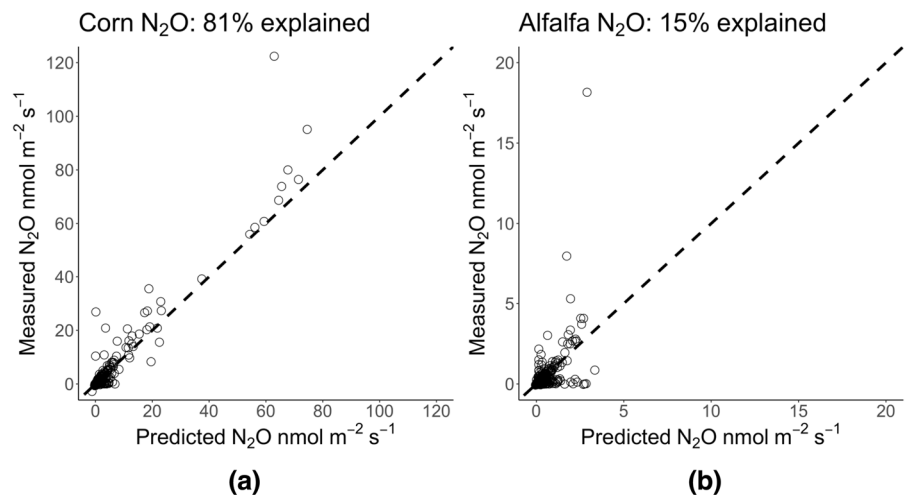
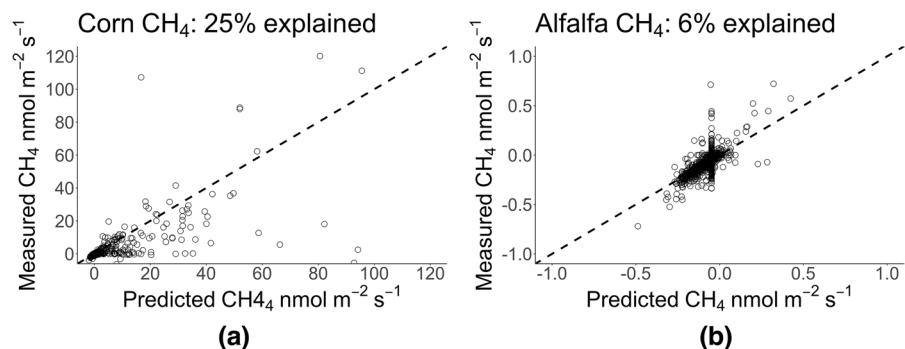


Fig. 7 Comparison of observed CH_4 fluxes ($\text{nmol m}^{-2} \text{s}^{-1}$) to machine learning predicted CH_4 fluxes ($\text{nmol m}^{-2} \text{s}^{-1}$) from agricultural peatland corn (a) and (b) alfalfa agroecosystems. Predictor variables were identical for each ecosystem (10, 30, and 50 cm depths with oxygen, moisture, and temperature sensors)



season, year) that vary over space and time. It is well known that the rates and reactions of biogeochemical processes can vary greatly in space and time, and it is often postulated that similar mechanisms drive the occurrence of both hot spots and hot moments (McClain et al. 2003; Bernhardt et al. 2017). This often leads to the assumption that hot spot and hot moment phenomena occur at similar rates for these biogeochemical processes, thus exhibiting similar influences on elemental cycles and ecosystem greenhouse gas budgets. Here we found that the occurrence and magnitude of hot spots and hot moments of CO₂, CH₄, and N₂O fluxes were not consistent across time or space, were not consistently distributed across ecosystems, and differed by gas. Hot moments of N₂O fluxes were common across chambers in both the corn and alfalfa sites, and hot spots of emissions differed across the years in the two longer term datasets. In the pasture, there was a single hot spot of N₂O emissions that accounted for 69% of the hot moments over the 1-year study period. Interestingly, the most productive hot spots of N₂O emissions occurred primarily in the same chambers as high CO₂ emission at all sites. This may indicate that these hot spots have high labile C availability and organic matter mineralization rates, characteristics that can support both nitrifier denitrification and canonical denitrification (Firestone and Davidson 1989; Wallenstein et al. 2006). Methane hotspots were also tied to hot moments of emissions and were largely limited to a single chamber location in the corn site. The corn site had a single chamber with a disproportionate impact on total ecosystem fluxes. Patterns for CH₄ in alfalfa and pastures ecosystems were more variable over time.

Predicting hot spots and hot moments requires intensive sampling across scales

Historically, predictive N₂O and CH₄ models utilized controlling variables together with assumptions regarding rate constants and kinetics (Müller et al. 2007; Rütting and Müller 2007; Riley et al. 2011). Machine learning approaches are becoming more popular for predicting N₂O fluxes, but their wider application has been limited by the lack of sufficient within site replication and the high sampling frequencies of relevant variables across scales needed to effectively train models. Due to methodological limitations in how we measure greenhouse gas fluxes,

we are currently only able to measure these phenomena at limited scales in the field (either chamber- or eddy covariance-scales). Here we used datasets with 33,000 to 103,000 flux measurements at the chamber-scale. In the corn ecosystem, VWC and temperature across depths had the highest relative importance in determining N₂O fluxes, similar to previous observations using wavelet coherence analyses (Anthony and Silver 2021). The lower predictability of N₂O fluxes observed in the alfalfa ecosystem and unexplained variance in the corn system may be due to low spatial resolution of the sensor measurements and underfitting of hot moments of emissions. Both systems only had two sets of sensors per field and were installed at 10, 30, and 50 cm depths, which may or may not have corresponded to locations where hot moments of N₂O production occurred, and the spatiotemporal controls on them may be more variable across a field. As both machine learning models systematically underfit the largest N₂O hot moments, this is likely representative of the unaccounted spatial and temporal variance driving these extreme hot moments in both models. This underfitting may be occurring if the input soil variables are not capturing the spatiotemporal variability, and/or our limited spatial resolution during hot moment observations.

In both the pasture and alfalfa sites a low number of significant CH₄ hot moments, such as those observed in wetlands or thawing permafrost (Elder et al. 2021; Rey-Sanchez et al. 2022a), is not surprising as these land uses are predominantly drained throughout the year. There are several potential explanations for the poor CH₄ model performance in the machine learning models used here. First, some other unmeasured variable, such as C substrate availability or the presence of reducible Fe or sulfate species, could be a strong driver of soil CH₄ flux (Chamberlain et al. 2018, 2019). Another potential explanation may be that there was insufficient spatial coverage of soil profile measurements of O₂, temperature, and VWC. This would suggest that increasing spatial measurements of the variables controlling CH₄ hot spots, potentially alongside each individual chamber, is needed to appropriately quantify the variables controlling the spatial variability in CH₄ fluxes at the chamber scale observed.

Combining chamber-based measurements with larger scale measurements (such as eddy covariance) may help to better constrain the spatiotemporal

drivers of ecosystem-scale variability. High density eddy covariance-based measurements have significantly increased the amount and availability of ecosystem-scale CH_4 flux datasets (Knox et al. 2019; Delwiche et al. 2021). These eddy covariance datasets have also highlighted the increased ability to determine time-scale emergent drivers at ecosystem scales (Sturtevant et al. 2016; Chamberlain et al. 2018). However, they are generally not able to measure the dynamics and controls of CH_4 fluxes at the spatial scales needed to accurately determine the distribution and drivers of hot spots and hot moments. Additionally, eddy covariance measurements of CH_4 have detection limits that are too high to accurately determine CH_4 consumption. Eddy covariance measurements alongside chamber measurements can provide insights to spatiotemporal variability of CH_4 fluxes and help determine their importance at the ecosystem-scale. Another approach that may improve the ability to model hot spots and hot moments utilizes eddy covariance flux measurements of CH_4 fluxes and footprint-weighted hot spot detection (Rey-Sanchez et al. 2022a) alongside automated chamber and soil sensor measurements at smaller scales to constrain the spatiotemporal distribution of CH_4 hot spots and hot moments. Unfortunately, current eddy covariance methods for N_2O measurements are often prohibitively expensive and have higher detection limits than chamber-based measurements (Tallec et al. 2019; O'Connell et al. 2022).

Drivers of nitrous oxide and methane hot spots

Drivers of soil greenhouse gas fluxes often vary across scales, from seconds (e.g., respiration) to years (e.g., succession) and from micrometers (e.g., soil aggregate) to kilometers (e.g., whole ecosystems) (Anthony et al. 2023). Interactions between soil O_2 availability, temperature, moisture, and substrate concentrations are thought to drive hot spots and hot moments of soil N_2O and CH_4 flux (Butterbach-Bahl et al. 2013; Nazaries et al. 2013; Pärn et al. 2018). The magnitude of soil N_2O and CH_4 fluxes also likely depends on the previous biogeochemical conditions as these will influence the composition of the microbial community and its response to events such as soil inundation or changes in substrate availability (Wallenstein et al. 2006). High rates of denitrification require both NO_3^- and labile C (Dietz and Clausen

2006). In contrast, methanogenesis, as a low-energy yielding oxidation–reduction reaction, is assumed to only occur in the absence of other electron acceptors under very low redox conditions (Conrad 1989). Thus, controls on the spatiotemporal availability of these substrates likely facilitate increased variability in hot spots and hot moments.

In agricultural peatlands, these variables are often controlled by both the rate and extent of soil drainage. The amount of time that peat soils are drained, the rate of soil inundation, and soil organic matter content are directly related to land use practices. The severity of peatland degradation determines economically viable land uses, but these land uses often lead to further peatland degradation (Leifeld et al. 2019, 2020). Corresponding land use and the extent of peatland degradation may also play a role in the magnitude of hot moments. Soil NO_3^- concentrations accumulate under oxic, well-drained soil conditions following soil organic N mineralization (Kirk et al. 2015; Anthony and Silver 2021), and the rate of accumulation is likely dependent on both the concentration of mineralizable organic matter and the amount of time and extent of soil drainage that provides optimal conditions for nitrification. In the corn agroecosystem, the elevated organic matter content and high organic matter mineralization rates coupled with extended periods of soil inundation were likely drivers of the magnitude of hot spots and hot moments (Anthony and Silver 2021). High C and NO_3^- substrate availability, along with spatiotemporal variability in redox conditions driven by variations in moisture, O_2 , and temperature, likely contributed to the distribution of hot spots and hot moments observed. The distribution of hot spots and hot moments in the alfalfa agroecosystem likely suggests that elevated N availability from alfalfa N-fixation and short-term changes in O_2 availability stimulated N_2O fluxes but did not produce redox conditions suitable for CH_4 production. In the degraded pasture, the ditched subsurface irrigation likely maintained anaerobic conditions throughout the soil profile, limiting hot moments of N_2O flux from incomplete denitrification. The patterns observed in the pasture agroecosystem were likely to be affected by the lower C substrate availability, which may help explain the spatiotemporal variation in CH_4 production and limited CH_4 hot moments. Combined, these results suggest variation in substrate availability, soil moisture content, flooding duration, and associated

effects on O₂ availability and soil redox conditions likely contribute to the variation in hot spots and hot moments observed across these agricultural peatland ecosystems. These differences also contribute to the variation in ecosystem greenhouse gas budgets and the effects of hot spots and hot moments on these budgets observed across the three land uses in this study.

The magnitude and distribution of hot spots and hot moments in agricultural peatlands vary across time and space

The findings reported here highlight the importance of hot moments in overall N₂O and CH₄ budgets in agricultural peatland soils. We found significant variability in hot spots of greenhouse gas fluxes over time and space. Hot spots (here defined as a location with a disproportionate number of hot moment observations) occurred in all three ecosystems but were generally not characterized by sustained high emissions from a single location, except in the pasture site with a shorter observation period. Hot spots were more commonly characterized by high proportion of hot moments in single changes over time, or high emissions from different chambers that varied within and across years. Variability in the controls on greenhouse gas fluxes, such as soil moisture, soil O₂, and substrate availability are likely driving these differences. However, poor spatiotemporal resolution of these variables or other potential unmeasured drivers are likely limiting our ability to predict the occurrence of hot spots and hot moments. Given the elevated substrate availability and predictable management-induced changes in soil redox conditions in many agricultural peatland soils, they are an ideal place to study the biogeochemical processes controlling greenhouse gas fluxes. Quantifying the drivers of this variability in agricultural peatland soils will greatly improve our understanding of the processes, controls, and distribution of hot spots and hot moments of greenhouse gas fluxes and improve land management decisions that to help mitigate climate change. Given the significant variability in hot spots and hot moments across agricultural peatland ecosystems, spatiotemporally intensive measurements of CO₂, CH₄, and N₂O fluxes and their associated drivers are needed to appropriately constrain their respective greenhouse gas budgets. Emerging technologies are dramatically increasing

soil sensor capabilities while simultaneously decreasing per sensor cost (e.g., Baumbauer et al. 2022). This can help us improve both sampling density and sampling frequency, allowing us to capture the drivers of greenhouse gas fluxes across spatial and temporal scales. Overall, these findings contribute to a better understanding of the biogeochemical patterns and pathways of soil greenhouse gas fluxes in agricultural peatland soils, highlight the considerable variability in hot spot and hot moment emissions across space and time, and the need for datasets with increased spatiotemporal resolution of both N₂O, and CH₄ fluxes and their controls to properly model ecosystem-scale fluxes.

Acknowledgements The authors appreciate assistance from Gisela Gonzalez, Heather Dang, Tibisay Pérez, and numerous other members of both the Silver Lab and the Berkeley Biometeorology Lab at the University of California, Berkeley. The concept for this paper was developed at the workshop titled "Peatlands for climate change mitigation in agriculture" that took place in Aarhus, Denmark, on 4-5 October 2022, and which was sponsored by the Organisation for Economic Co-operation and Development (OECD) Co-operative Research Programme: Sustainable Agricultural and Food Systems. The opinions expressed and arguments employed in this publication are the sole responsibility of the authors and do not necessarily reflect those of the OECD or of the governments of its Member countries.

Author contributions All authors contributed to the study conception and design. Material preparation, data collection and analysis were performed by TLA. The first draft of the manuscript was written by TLA and WLS. All authors read and approved the final manuscript. McIntire Stennis grant CA-B-ECO-7673-MS to WLS partially supported this work. W. L. Silver was also supported by funds from breakthrough strategies & solutions, and the VKR, OC, Jewish Community, Northern Trust, and Trisons Foundations.

Funding This work was supported by a Contract by the California Department of Water Resources (award 4600011240). We thank the California Department of Water Resources and the Metropolitan Water District of Southern California for research site access. T. L. Anthony was supported by the California Sea Grant Delta Science Fellowship. This material is based upon the work supported by the Delta Stewardship Council Delta Science Program under Grant No. 5298 and California Sea Grant College Program Project R/SF-89. The contents of this material do not necessarily reflect the views and policies of the Delta Stewardship Council, nor does mention of trade names or commercial products constitute endorsement or recommendation for use.

Data availability The daily mean greenhouse gas fluxes by chamber (chamber CO₂, CH₄, N₂O, and eddy covariance CO₂), and soil O₂, temperature, and moisture sensor data in this study

will be deposited in the Dryad database: <https://doi.org/10.5061/dryad.qz612jmnx>

Declarations

Competing interests The authors declare no conflict of interests.

Open Access This article is licensed under a Creative Commons Attribution 4.0 International License, which permits use, sharing, adaptation, distribution and reproduction in any medium or format, as long as you give appropriate credit to the original author(s) and the source, provide a link to the Creative Commons licence, and indicate if changes were made. The images or other third party material in this article are included in the article's Creative Commons licence, unless indicated otherwise in a credit line to the material. If material is not included in the article's Creative Commons licence and your intended use is not permitted by statutory regulation or exceeds the permitted use, you will need to obtain permission directly from the copyright holder. To view a copy of this licence, visit <http://creativecommons.org/licenses/by/4.0/>.

References

- Adewale C, Higgins S, Granatstein D et al (2016) Identifying hotspots in the carbon footprint of a small scale organic vegetable farm. *Agric Syst* 149:112–121. <https://doi.org/10.1016/j.agsy.2016.09.004>
- Alber M, Buganza Tepole A, Cannon WR et al (2019) Integrating machine learning and multiscale modeling—perspectives, challenges, and opportunities in the biological, biomedical, and behavioral sciences. *Npj Digit Med* 2:1–11. <https://doi.org/10.1038/s41746-019-0193-y>
- Anthony TL, Silver WL (2020) Mineralogical associations with soil carbon in managed wetland soils. *Glob Chang Biol* 26:6555–6567. <https://doi.org/10.1111/gcb.15309>
- Anthony TL, Silver WL (2021) Hot moments drive extreme nitrous oxide and methane emissions from agricultural peatlands. *Glob Chang Biol*. <https://doi.org/10.1111/gcb.15802>
- Anthony TL, Szutu DJ, Verfaillie JG et al (2023) Carbon-sink potential of continuous alfalfa agriculture lowered by short-term nitrous oxide emission events. *Nat Commun* 14:1926. <https://doi.org/10.1038/s41467-023-37391-2>
- Barton L, Wolf B, Rowlings D et al (2015) Sampling frequency affects estimates of annual nitrous oxide fluxes. *Sci Rep* 5:1–9. <https://doi.org/10.1038/srep15912>
- Baumbauer CL, Goodrich PJ, Payne ME, Anthony T, Beckstoffer C, Toor A, Silver W, Arias AC (2022) Printed potentiometric nitrate sensors for use in soil. *Sensors* 22(11):4095
- Baveye PC, Otten W, Kravchenko A et al (2018) Emergent properties of microbial activity in heterogeneous soil microenvironments: different research approaches are slowly converging, yet major challenges remain. *Front Microbiol* 9:1929
- Bernhardt ES, Blaszczak JR, Ficken CD et al (2017) Control points in ecosystems: moving beyond the hot spot hot moment concept. *Ecosystems* 20:665–682. <https://doi.org/10.1007/s10021-016-0103-y>
- Breiman L (2001) Random forests. *Mach Learn* 45:5–32. <https://doi.org/10.1023/A:1010933404324>
- Buschmann C, Röder N, Berglund K et al (2020) Land Use Policy Perspectives on agriculturally used drained peat soils: comparison of the socioeconomic and ecological business environments of six European regions. *Land Use Policy* 90:104181. <https://doi.org/10.1016/j.landusepol.2019.104181>
- Butterbach-Bahl K, Baggs EM, Dannenmann M et al (2013) Nitrous oxide emissions from soils: how well do we understand the processes and their controls? *Philos Trans R Soc Lond Ser B* 368:20130122. <https://doi.org/10.1098/rstb.2013.0122>
- Carlson KM, Gerber JS, Mueller ND et al (2017) Greenhouse gas emissions intensity of global croplands. *Nat Clim Chang* 7:63–68. <https://doi.org/10.1038/nclimate3158>
- Carter RE (2013) A standard error: distinguishing standard deviation from standard error. *Diabetes* 62:e15. <https://doi.org/10.2337/db13-0692>
- Chamberlain SD, Anthony TL, Silver WL et al (2018) Soil properties and sediment accretion modulate methane fluxes from restored wetlands. *Glob Chang Biol* 24:4107–4121. <https://doi.org/10.1111/gcb.14124>
- Chamberlain SD, Hemes KS, Eichelmann E et al (2019) Effect of drought-induced salinization on wetland methane emissions, gross ecosystem productivity, and their interactions. *Ecosystems*. <https://doi.org/10.1007/s10021-019-00430-5>
- Chatskikh D, Olesen JE, Berntsen J et al (2005) Simulation of effects of soils, climate and management on N₂O emission from grasslands. *Biogeochemistry* 76:395–419. <https://doi.org/10.1007/s10533-005-6996-8>
- Conrad R (2007) Microbial ecology of methanogens and methanotrophs. *Adv Agron* 96:1–63. [https://doi.org/10.1016/S0065-2113\(07\)96005-8](https://doi.org/10.1016/S0065-2113(07)96005-8)
- Conrad R (1989) Control of methane production in terrestrial ecosystems. Exchange of trace gases between terrestrial ecosystems and the atmosphere. Wiley, New York, pp 39–58
- Danevčič T, Mandić-Mulec I, Stres B et al (2010) Emissions of CO₂, CH₄ and N₂O from Southern European peatlands. *Soil Biol Biochem* 42:1437–1446. <https://doi.org/10.1016/j.soilbio.2010.05.004>
- Delwiche KB, Knox SH, Malhotra A et al (2021) FLUXNET-CH₄: a global, multi-ecosystem dataset and analysis of methane seasonality from freshwater wetlands. *Earth Syst Sci Data* 13:3607–3689. <https://doi.org/10.5194/essd-13-3607-2021>
- Dietz ME, Clausen JC (2006) Saturation to improve pollutant retention in a rain garden. *Environ Sci Technol* 40:1335–1340. <https://doi.org/10.1021/es051644f>
- Ehrhardt F, Soussana J-F, Bellocchi G et al (2018) Assessing uncertainties in crop and pasture ensemble model simulations of productivity and N₂O emissions. *Glob Chang Biol* 24:e603–e616. <https://doi.org/10.1111/gcb.13965>
- Eichelmann E, Hemes KS, Knox SH et al (2018) The effect of land cover type and structure on evapotranspiration from agricultural and wetland sites in the Sacramento/

- San Joaquin River Delta, California. *Agric For Meteorol* 256–257:179–195. <https://doi.org/10.1016/j.agrformet.2018.03.007>
- Elder CD, Thompson DR, Thorpe AK et al (2021) Characterizing methane emission hotspots from thawing permafrost. *Glob Biogeochem Cycles* 35:e2020GB006922. <https://doi.org/10.1029/2020GB006922>
- Feng J, Yang T, Li F et al (2021) Impact of tillage on the spatial distribution of CH₄ and N₂O in the soil profile of late rice fields. *Soil Tillage Res* 211:105029. <https://doi.org/10.1016/j.still.2021.105029>
- Firestone MK, Davidson EA (1989) Microbiological Basis of NO and N₂O production and consumption in soil. *Exchange Trace Gases Terr Ecosyst Atmos*. <https://doi.org/10.1017/CBO9781107415324.004>
- Freeman BWJ, Evans CD, Musarika S et al (2022) Responsible agriculture must adapt to the wetland character of mid-latitude peatlands. *Glob Chang Biol* 28:3795–3811. <https://doi.org/10.1111/gcb.16152>
- Gaillard RK, Jones CD, Ingraham P et al (2018) Underestimation of N₂O emissions in a comparison of the DayCent, DNDC, and EPIC models. *Ecol Appl* 28:694–708. <https://doi.org/10.1002/eap.1674>
- Golovchenko AV, Tikhonova EY, Zvyagintsev DG (2007) Abundance, biomass, structure, and activity of the microbial complexes of minerotrophic and ombrotrophic peatlands. *Microbiology* 76:630–637. <https://doi.org/10.1134/S0026261707050177>
- Günther A, Barthelmes A, Huth V et al (2019) Prompt rewetting of drained peatlands reduces climate warming despite methane emissions. *bioRxiv preprint* 1–13
- Hall SJ, Tenesaca CG, Lawrence NC et al (2023) Poorly drained depressions can be hotspots of nutrient leaching from agricultural soils. *J Environ Qual* 52:678–690. <https://doi.org/10.1002/jeq2.20461>
- Hamrani A, Akbarzadeh A, Madramootoo CA (2020) Machine learning for predicting greenhouse gas emissions from agricultural soils. *Sci Total Environ* 741:140338. <https://doi.org/10.1016/j.scitotenv.2020.140338>
- Hatala JA, Detto M, Sonnentag O et al (2012) Greenhouse gas (CO₂, CH₄, H₂O) fluxes from drained and flooded agricultural peatlands in the Sacramento-San Joaquin Delta. *Agric Ecosyst Environ* 150:1–18. <https://doi.org/10.1016/j.agee.2012.01.009>
- Hemes KS, Chamberlain SD, Eichelmann E et al (2019) Assessing the carbon and climate benefit of restoring degraded agricultural peat soils to managed wetlands. *Agric For Meteorol* 268:202–214. <https://doi.org/10.1016/j.agrformet.2019.01.017>
- Holst J, Liu C, Yao Z et al (2008) Fluxes of nitrous oxide, methane and carbon dioxide during freezing–thawing cycles in an Inner Mongolian steppe. *Plant Soil* 308:105–117. <https://doi.org/10.1007/s11104-008-9610-8>
- Jerman V, Danevčič T, Mandić-Mulec I (2017) Methane cycling in a drained wetland soil profile. *J Soils Sediments* 17:1874–1882. <https://doi.org/10.1007/s11368-016-1648-2>
- Jobbagy EG, Jackson RB (2000) The vertical distribution of soil organic carbon and its relation to climate and vegetation. *Ecol Appl* 10:423–436
- Kasak K, Camilo R-S, Szutu D, Baldocchi D (2020) AmeriFlux BASE US-Snf Sherman Barn
- Kirk ER, Van Kessel C, Horwath WR, Linnquist BA (2015) Estimating annual soil carbon loss in agricultural peatland soils using a nitrogen budget approach. *PLoS ONE* 10:1–18. <https://doi.org/10.1371/journal.pone.0121432>
- Knox SH, Jackson RB, Poulter B et al (2019) FLUXNET-CH₄ synthesis activity: objectives, observations, and future directions. *Bull Am Meteor Soc* 100:2607–2632. <https://doi.org/10.1175/BAMS-D-18-0268.1>
- Knox SH, Sturtevant C, Matthes JH et al (2015) Agricultural peatland restoration: effects of land-use change on greenhouse gas (CO₂ and CH₄) fluxes in the Sacramento-San Joaquin Delta. *Glob Chang Biol* 21:750–765. <https://doi.org/10.1111/gcb.12745>
- Krichels AH, DeLucia EH, Sanford R et al (2019a) Historical soil drainage mediates the response of soil greenhouse gas emissions to intense precipitation events. *Biogeochemistry* 142:425–442. <https://doi.org/10.1007/s10533-019-00544-x>
- Krichels AH, Sipic E, Yang WH (2019b) Iron redox reactions can drive microtopographic variation in upland soil carbon dioxide and nitrous oxide emissions. *Soil Syst* 3:1–16. <https://doi.org/10.3390/soilsystems3030060>
- Krichels AH, Yang WH (2019) Dynamic controls on field-scale soil nitrous oxide hot spots and hot moments across a microtopographic gradient. *J Geophys Res Biogeosci* 124:3618–3634. <https://doi.org/10.1029/2019JG005224>
- Leifeld J, Klein K, Wüst-Galley C (2020) Soil organic matter stoichiometry as indicator for peatland degradation. *Sci Rep* 10:1–9. <https://doi.org/10.1038/s41598-020-64275-y>
- Leifeld J, Menichetti L (2018) The underappreciated potential of peatlands in global climate change mitigation strategies. *Nat Commun*. <https://doi.org/10.1038/s41467-018-03406-6>
- Leifeld J, Wüst-Galley C, Page S (2019) Intact and managed peatland soils as a source and sink of GHGs from 1850 to 2100. *Nat Clim Chang* 9:945–947. <https://doi.org/10.1038/s41558-019-0615-5>
- Maljanen M, Sigurdsson BD, Guömundsson J et al (2010) Greenhouse gas balances of managed peatlands in the Nordic countries present knowledge and gaps. *Biogeosciences* 7:2711–2738. <https://doi.org/10.5194/bg-7-2711-2010>
- Martikainen PJ, Nykänen H, Crill P, Silvola J (1993) Effect of a lowered water table on nitrous oxide fluxes from northern peatlands. *Nature* 366:51–53. <https://doi.org/10.1038/366051a0>
- McClain ME, Boyer EW, Dent CL et al (2003) Biogeochemical hot spots and hot moments at the interface of terrestrial and aquatic ecosystems. *Ecosystems* 6:301–312. <https://doi.org/10.1007/s10021-003-0161-9>
- McNicol G, Silver WL (2014) Separate effects of flooding and anaerobiosis on soil greenhouse gas emissions and redox sensitive biogeochemistry. *J Geophys Res Biogeosci* 119:557–566. <https://doi.org/10.1002/2013JG002433>
- Molodovskaya M, Singurindy O, Richards BK et al (2012) Temporal variability of nitrous oxide from fertilized croplands: hot moment analysis. *Soil Sci Soc Am J* 76:1728. <https://doi.org/10.2136/sssaj2012.0039>

- Müller C, Rütting T, Kattge J et al (2007) Estimation of parameters in complex 15N tracing models by Monte Carlo sampling. *Soil Biol Biochem* 39:715–726. <https://doi.org/10.1016/j.soilbio.2006.09.021>
- Myhre G, Shindell D, Bréon F-M et al (2013) Anthropogenic and Natural Radiative Forcing. *Climate Change 2013: The Physical Science Basis Contribution of Working Group I to the Fifth Assessment Report of the Intergovernmental Panel on Climate Change*, pp 659–740. <https://doi.org/10.1017/CBO9781107415324.018>
- Nazaries L, Murrell JC, Millard P et al (2013) Methane, microbes and models: fundamental understanding of the soil methane cycle for future predictions. *Environ Microbiol* 15:2395–2417. <https://doi.org/10.1111/1462-2920.12149>
- O’Connell CS, Anthony TL, Mayes MA, Pérez T, Sihi D, Silver WL (2022) Utilizing novel field and data exploration methods to explore hot moments in high-frequency soil nitrous oxide emissions data: opportunities and challenges. *Front For Glob Chang* 5:674348
- Oikawa PY, Jenerette GD, Knox SH et al (2017) Evaluation of a hierarchy of models reveals importance of substrate limitation for predicting carbon dioxide and methane exchange in restored wetlands. *J Geophys Res Biogeosci* 122:145–167. <https://doi.org/10.1002/2016JG003438>
- Oktarita S, Hergoualc’H K, Anwar S, Verchot LV (2017) Substantial N₂O emissions from peat decomposition and N fertilization in an oil palm plantation exacerbated by hotspots. *Environ Res Lett*. <https://doi.org/10.1088/1748-9326/aa80f1>
- Pärn J, Verhoeven JTA, Butterbach-Bahl K et al (2018) Nitrogen-rich organic soils under warm well-drained conditions are global nitrous oxide emission hotspots. *Nat Commun* 9:1–8. <https://doi.org/10.1038/s41467-018-03540-1>
- Pellerin B, Anderson FE, Bergamaschi B (2014) Assessing the role of winter flooding on baseline greenhouse gas fluxes from corn fields in the Sacramento-San Joaquin Bay Delta
- Potter CS (1997) An ecosystem simulation model for methane production and emission from wetlands. *Global Biogeochem Cycles* 11:495–506. <https://doi.org/10.1029/97GB02302>
- Qiu J, Wu Q, Ding G et al (2016) A survey of machine learning for big data processing. *EURASIP J Adv Signal Process* 2016:67. <https://doi.org/10.1186/s13634-016-0355-x>
- Rey-Sanchez C, Arias-Ortiz A, Kasak K et al (2022) Detecting hot spots of methane flux using footprint-weighted flux maps. *J Geophys Res* 127:e2022JG006977. <https://doi.org/10.1029/2022JG006977>
- Rey-Sanchez C, Szutu D, Baldocchi D, Hemes K (2021) AmeriFlux US-Bi2 Bouldin Island corn
- Rey-Sanchez C, Wang CT, Szutu D, et al (2022b) AmeriFlux BASE US-Bi1 Bouldin Island Alfalfa
- Riley WJ, Subin ZM, Lawrence DM et al (2011) Barriers to predicting changes in global terrestrial methane fluxes: analyses using CLM4Me, a methane biogeochemistry model integrated in CESM. *Biogeosciences* 8:1925–1953. <https://doi.org/10.5194/bg-8-1925-2011>
- Rütting T, Müller C (2007) 15N tracing models with a Monte Carlo optimization procedure provide new insights on gross N transformations in soils. *Soil Biol Biochem* 39:2351–2361. <https://doi.org/10.1016/j.soilbio.2007.04.006>
- Saha D, Basso B, Robertson GP (2021) Machine learning improves predictions of agricultural nitrous oxide (N₂O) emissions from intensively managed cropping systems. *Environ Res Lett*. <https://doi.org/10.1088/1748-9326/abd2f3>
- Savage K, Phillips R, Davidson E (2014) High temporal frequency measurements of greenhouse gas emissions from soils. *Biogeosciences* 11:2709–2720. <https://doi.org/10.5194/bg-11-2709-2014>
- Segal M, Xiao Y (2011) Multivariate random forests. *Wires Data Min Knowl Discov* 1:80–87. <https://doi.org/10.1002/widm.12>
- Sokol NW, Slessarev E, Marschmann GL et al (2022) Life and death in the soil microbiome: how ecological processes influence biogeochemistry. *Nat Rev Microbiol* 20:415–430. <https://doi.org/10.1038/s41579-022-00695-z>
- Sturtevant C, Ruddell BL, Knox SH et al (2016) Identifying scale-emergent, nonlinear, asynchronous processes of wetland methane exchange. *J Geophys Res Biogeosci* 121:188–204. <https://doi.org/10.1002/2015JG003054>
- Talleg T, Brut A, Joly L et al (2019) N₂O flux measurements over an irrigated maize crop: a comparison of three methods. *Agric For Meteorol* 264:56–72. <https://doi.org/10.1016/j.agrformet.2018.09.017>
- Teh YA, Silver WL, Sonnentag O et al (2011) Large greenhouse gas emissions from a temperate peatland pasture. *Ecosystems* 14:311–325. <https://doi.org/10.1007/s10021-011-9411-4>
- The Delta Protection Commission (2020) *The State of Delta Agriculture : Economic Impact , Conservation and Trends*
- Thorup-Kristensen K, Halberg N, Nicolaisen M et al (2020) Digging deeper for agricultural resources, the value of deep rooting. *Trends Plant Sci* 25:406–417. <https://doi.org/10.1016/j.tplants.2019.12.007>
- Totsche KU, Rennert T, Gerzabek MH et al (2010) Biogeochemical interfaces in soil: the interdisciplinary challenge for soil science. *J Plant Nutr Soil Sci* 173:88–99. <https://doi.org/10.1002/jpln.200900105>
- Wagner-Riddle C, Congreves KA, Abalos D et al (2017) Globally important nitrous oxide emissions from croplands induced by freeze–thaw cycles. *Nat Geosci*. <https://doi.org/10.1038/ngeo2907>
- Wallenstein MD, Myrold DD, Firestone M, Voytek M (2006) Environmental controls on denitrifying communities and denitrification rates: insights from molecular methods. *Ecol Appl* 16:2143–2152. [https://doi.org/10.1890/1051-0761\(2006\)016\[2143:ECODCA\]2.0.CO;2](https://doi.org/10.1890/1051-0761(2006)016[2143:ECODCA]2.0.CO;2)
- Xing H, Wang E, Smith CJ et al (2011) Modelling nitrous oxide and carbon dioxide emission from soil in an incubation experiment. *Geoderma* 167–168:328–339. <https://doi.org/10.1016/j.geoderma.2011.07.003>
- Yang WH, Liptzin D (2015) High potential for iron reduction in upland soils. *Ecology* 96:2015–2020. <https://doi.org/10.1890/14-2097.1>
- Yang WH, Weber KA, Silver WL (2012) Nitrogen loss from soil through anaerobic ammonium oxidation coupled to iron reduction. *Nat Geosci*. <https://doi.org/10.1038/ngeo1530>

Publisher's Note Springer Nature remains neutral with regard to jurisdictional claims in published maps and institutional affiliations.